

Lattice QCD: The case of parton densities

The Ze-Ro Zeuthen-Roma Collaboration

M. Guagnelli¹, K. Jansen², F. Palombi¹, R. Petronzio¹, A. Shindler^{2,a}, and I. Wetzorke²

¹ Dipartimento di Fisica, Università di Roma Tor Vergata, INFN, Sezione di RomaII, Via della Ricerca Scientifica 1, I-00133 Rome, Italy

² Deutsches Elektronen-Synchrotron, DESY-Zeuthen, John von Neumann-Institut für Computing (NIC), Platanenallee 6, D-15738 Zeuthen, Germany

Received: 1 November 2002 /

Published online: 15 July 2003 – © Società Italiana di Fisica / Springer-Verlag 2003

Abstract. The accuracy of structure functions computations on the lattice may become comparable to experimental determinations. We discuss the strategy followed by the Ze-Ro Collaboration that allows the reconstruction of the running of the leading-twist non-singlet operator in the continuum and fully non-perturbatively renormalized.

PACS. 11.15.Ha Lattice gauge theory – 12.38.Gc Lattice QCD calculations

1 Introduction

Structure functions normalize the calculations of hard processes with hadrons in the initial state and large momentum transfers. The prototype of such processes is given by the Deep Inelastic Scattering (DIS) that is the inclusive inelastic collision between a lepton and a hadron. The cross-section of the process is the convolution of the “bare” cross-section between the lepton and a parton, and the Parton Distribution Function (PDF) $f_a(x)$. The PDF describes the probability to find a parton a with longitudinal fraction x of the hadron’s momentum. These densities teach us about the structure of hadrons. The cross-section for DIS

$$d\sigma \propto \frac{\alpha^2}{Q^4} L^{\mu\nu} W_{\mu\nu} \quad (1)$$

is in this case expressed in terms of a lepton tensor $L^{\mu\nu}(k, k')$ and a hadron tensor $W_{\mu\nu}(p, q)$,

$$\begin{aligned} L^{\mu\nu}(k, k') &= 2(k'^{\mu}k^{\nu} + k^{\mu}k'^{\nu}) - 2g^{\mu\nu}(k \cdot k'), \\ W_{\mu\nu}(p, q) &= \frac{1}{4\pi} \int d^4x e^{iqx} \langle h(p) | [J_{\mu}(x), J_{\nu}(0)] | h(p) \rangle, \end{aligned} \quad (2)$$

where $|h(p)\rangle$ is the hadronic state (pion, proton, ...), k and k' are the initial and the final momentum of the lepton, and $J_{\mu}(x)$ is the electromagnetic current. In the Bjorken limit, the hadronic tensor is dominated by the light cone contributions, $x^2 \sim 0$, and this prevents a direct calculation of $W_{\mu\nu}$ on a Euclidean lattice, necessary prerequisite for lattice QCD (LQCD). There are some very

preliminary attempts to compute directly on the lattice the product of the 2 electromagnetic currents, and relate this computation to the structure functions via a short-distance expansion [1]. However, we follow a standard approach. A light cone expansion allows to relate moments of the PDF $\langle x^{N-1} \rangle_a(Q) = M_a^{(N)}(Q)$,

$$M_a^{(N)}(Q = \mu) = \int_0^1 dx x^{N-1} [f_a(x, \mu) + (-1)^N f_{\bar{a}}(x, \mu)] \quad (3)$$

to expectations values of the local operator \mathcal{O}_a ,

$$M_a^{(N)}(\mu) p_{\mu_1} \cdots p_{\mu_N} = \langle h(p) | \mathcal{O}_{\mu_1 \cdots \mu_N}^a(\mu) | h(p) \rangle. \quad (4)$$

The operators are classified according to their twist τ (leading-twist operators have $\tau = 2$) and their flavour quantum numbers (flavour symmetry is a good symmetry if $Q^2 \rightarrow \infty$). The quark non-singlet operator is

$$\mathcal{O}_{\mu_1 \cdots \mu_N}^{qNS} = \frac{1}{2^N} \bar{\psi} \gamma_{[\mu_1} D_{\mu_2} \cdots D_{\mu_N]} \frac{\lambda^f}{2} \psi - \text{trace terms}, \quad (5)$$

and the quark and gluon singlet operators are

$$\begin{aligned} \mathcal{O}_{\mu_1 \cdots \mu_N}^{qS} &= \frac{1}{2^N} \bar{\psi} \gamma_{[\mu_1} D_{\mu_2} \cdots D_{\mu_N]} \psi - \text{trace terms}, \\ \mathcal{O}_{\mu_1 \cdots \mu_N}^{gS} &= \sum_{\rho} \text{Tr} \left\{ F_{[\mu_1 \rho} D_{\mu_2} \cdots D_{\mu_{N-1}} F_{\rho \mu_N]} \right\} \\ &\quad - \text{trace terms}, \end{aligned} \quad (6)$$

where D_{μ} is a covariant derivative and $[\cdots]$ means symmetrization on the Lorentz indices. Other interesting

^a Spokesperson; e-mail: shindler@ihf.de

quantities can be computed on the lattice like the moments of the spin-dependent structure functions g_1 and g_2 , and moments of the transversity structure function h_1 (preliminary results can be found in [2, 3]).

2 Lattice QCD

Euclidean space-time is replaced by a 4-dimensional hypercubic lattice. In the theory in the continuum, expectation values are expressed in terms of functional integrals over continuum fields:

$$\langle \Gamma \rangle = \frac{1}{\mathcal{Z}} \int \mathcal{D}[A] \mathcal{D}[\bar{\psi}] \mathcal{D}[\psi] \Gamma[A, \bar{\psi}, \psi] e^{-S[A, \bar{\psi}, \psi]}. \quad (7)$$

In numerical simulations, they are suitable to a lattice and correlation functions are obtained from averages of properly sampled lattice field configurations:

$$\langle \Gamma \rangle = \lim_{N_{\text{conf}} \rightarrow \infty} \frac{1}{N_{\text{conf}}} \sum_{N_{\text{conf}}} \Gamma[\text{conf}]. \quad (8)$$

The lattice Wilson-Dirac operator is given by

$$D_{\text{W}} = \frac{1}{2} \{ \gamma_{\mu} (\nabla_{\mu}^* + \nabla_{\mu}) - a \nabla_{\mu}^* \nabla_{\mu} \}, \quad (9)$$

where the forward and the backward derivatives are

$$\begin{aligned} \nabla_{\mu} \psi(x) &= \frac{1}{a} [U(x, \mu) \psi(x + a\hat{\mu}) - \psi(x)], \\ \nabla_{\mu}^* \psi(x) &= \frac{1}{a} [\psi(x) - U(x - a\hat{\mu}, \mu)^{-1} \psi(x - a\hat{\mu})]. \end{aligned} \quad (10)$$

The QCD action on the lattice may now be written in the form

$$S = \frac{1}{g_0^2} \sum_p \text{Tr} \{ 1 - U(p) \} + a^4 \sum_x \bar{\psi}(x) [D_{\text{W}} + m_0] \psi(x). \quad (11)$$

The sum in the gauge field part of the action runs over all oriented plaquettes p and $U(p)$ denotes the product of the gauge field variables around p :

$$U(p) = U(x, \mu) U(x + \hat{\mu}, \nu) U(x + \hat{\nu}, \mu)^{-1} U(x, \nu)^{-1}. \quad (12)$$

The Wilson term in the fermionic part of the action ($a \nabla_{\mu}^* \nabla_{\mu}$) is necessary to remove the ‘‘doublers’’, but unfortunately it breaks chiral symmetry even in the massless theory. For technical reasons, the matrix elements can be simulated only in a region of the quark masses that corresponds to $m_{\pi} \geq 500$ MeV. One needs then to perform a chiral extrapolation for quantities like the moments of the PDF, and this can be a source of systematic errors. A recent formulation of chiral fermions on the lattice [4] (overlap [5], domain-wall [6], fixed point [7]) may reduce these systematic uncertainties. However, they are very expensive to simulate. On the lattice the Grassmann variables are integrated out, and one then has

$$\mathcal{Z} = \int \mathcal{D}[U] \det(D_{\text{W}}[U] + m_0) e^{-S_g[U]}. \quad (13)$$

It is faster and not so far from real world to do the simulation with $\det(D_{\text{W}}[U] + m_0) = 1$. This approximation is called *quenching*. This means there are no sea quarks in the calculations: the internal quark loops are neglected. Lattice computations, like normal experiments, are affected by statistical and systematic errors. The statistical errors can be reduced, in principle, increasing the statistics. The main sources of systematic errors are: 1) discretization of the space-time; 2) perturbative renormalization; 3) chiral extrapolation; 4) quenching. Usually, the continuum limit is reached with a rate proportional to a , but convergence can be improved by modifying the definition of the lattice action $S[U, \bar{\psi}, \psi]$ and of the observable Γ by the addition of terms that naively go to zero in the continuum limit and cancel certain lattice artifacts:

$$\begin{aligned} - \text{before improvement,} \quad \langle \Gamma \rangle &= \Gamma_0 + a\Gamma_1 + a^2\Gamma_2 + O(a^3); \\ - \text{after improvement,} \quad \langle \Gamma \rangle &= \Gamma_0 + a^2\Gamma'_2 + O(a^3). \end{aligned} \quad (14)$$

3 Non-perturbative renormalization

The Ze-Ro Collaboration aims at solving 2 of the possible sources of systematic uncertainties: first, following the scale evolution of the local operator fully non-perturbatively and second, performing a well-controlled continuum limit [8–12]. Local operators need to be renormalized. In the non-singlet case there is no mixing between quark and gluon operators and we can write

$$\mathcal{O}_R(\mu) = Z_{\mathcal{O}}(a\mu) \mathcal{O}_{\text{bare}}(a). \quad (15)$$

Renormalization has to be done at some scale μ where perturbative calculations provide the determination of moments of parton densities from experimental data. But the hadron matrix elements must be able to feel the distances related to the hadronic bound state governed by a non-perturbative scale ($\sim \Lambda_{\text{QCD}}$). One can hardly accommodate on a single lattice a large ratio of scales ($\frac{\mu_{\text{ph}}}{\Lambda_{\text{QCD}}} \sim 100$) with negligible lattice artifacts. One should be able to renormalize at a strong interaction scale and then calculate a non-perturbative evolution up to a perturbative scale where contact with perturbation theory, and hence with the experiment, can be made. The strategy pioneered by the Alpha Collaboration [13] is to use a finite-size renormalization scheme called Schrödinger Functional (SF) scheme.

3.1 Schrödinger Functional

Every renormalization scheme on the lattice must satisfy general properties like: 1) it must be possible to change easily the renormalization scale; 2) the scheme has to guarantee a good numerical signal. The Schrödinger Functional is a finite-volume scheme that satisfies both these requirements. QCD is set up on a volume $T \times L^3$ with periodic boundary condition in spatial directions and Dirichlet boundary conditions in time. The finite extent L is used as

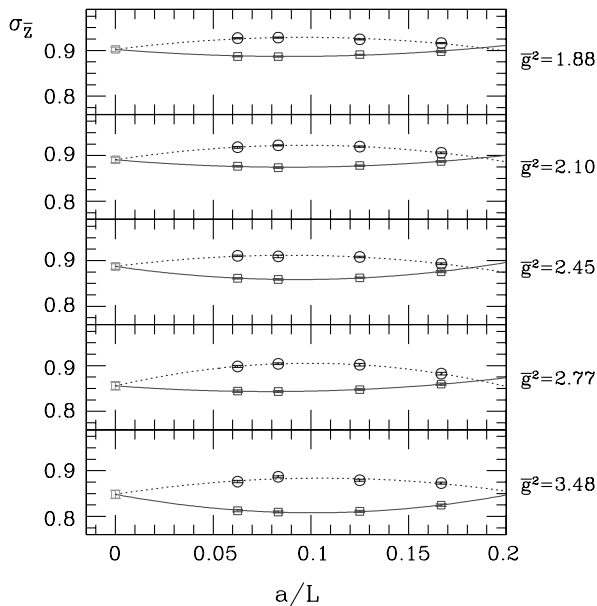


Fig. 1. Continuum limit of the lattice SSF for two ways of discretizing fermions on the lattice.

the renormalization scale $\mu = 1/L$, thus the finite-volume extent is a probe for the physics taking place at this scale. The continuum limit is performed letting $a \rightarrow 0$ at fixed L , but of course it is not possible to perform the continuum limit of the renormalization constant itself, that would diverge. The crucial ingredient is the so-called Step-Scaling Function (SSF). Assuming that we have renormalized a matrix element at a certain scale μ_0 , then the matrix element at a different scale μ will be given by

$$\mathcal{O}_R(\mu) = \sigma(\mu/\mu_0)\mathcal{O}_R(\mu_0), \quad (16)$$

where $\sigma(\mu/\mu_0) = Z_{\text{SF}}(\mu_0)/Z_{\text{SF}}(\mu)$ is the SSF. The SSF describes the full scale evolution of the scale-dependent quantity of interest. Different observables need a different SSF. A very important property of the SSF is that it can be split into several steps. Identifying the scale $\mu = 1/L$ and choosing steps of size 2 we have

$$\sigma(L_0/L) = \sigma(2L/L)\sigma(4L/2L) \cdots \sigma(L_0/(L_0/2)). \quad (17)$$

The aim is to have the SSFs of eq. (17) non-perturbatively and in the continuum. An important remark is that the SSF $\sigma(2L/L)$ has indeed a well-defined continuum limit such that the whole procedure makes sense. On the lattice we introduce the lattice SSF

$$\Sigma(a) = \sigma(2L/L, a). \quad (18)$$

$\Sigma(a)$ is the quantity that can be computed on the lattice. The continuum SSF is then reached through

$$\sigma = \lim_{a \rightarrow 0} \Sigma(a) \Big|_{\mu^{-1} = L \text{ fixed}}. \quad (19)$$

In the $a \rightarrow 0$ limit, the physical scale L is kept fixed. This can be achieved by fixing the value of the renormalized

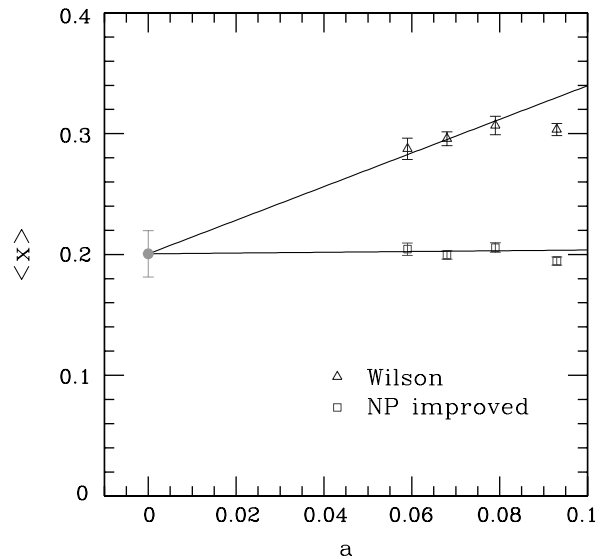


Fig. 2. Continuum limit of the renormalized matrix element for two ways of discretizing fermions on the lattice.

gauge coupling \bar{g} . In fig. 1 we show the approach to the continuum limit of $\Sigma(a)$ (18), for two ways of discretizing fermions on the lattice, one with standard fermions (dashed lines) using the action of eq. (11) and a non-perturbatively improved action (full lines). Both Σ 's extrapolate to the same SSF showing the universality of the continuum limit. The individual plots are obtained at fixed values of the running coupling \bar{g} corresponding to a fixed scale $1/L$. Figure 1 demonstrates that the approach to the continuum limit of the lattice SSF is well controlled. The second important ingredient is the computation of the renormalized matrix element at a non-perturbative scale μ_0 where finite-volume effects are negligible. This can be done by computing the bare matrix element of the local operator between hadron states (pions in our case), and the renormalization constant at the same bare coupling g_0 . Then it is possible to do a continuum and chiral extrapolation, at the fixed scale μ_0 . In fig. 2 we show the continuum limit of the renormalized matrix element with two different lattice fermionic actions. Putting together, following eq. (16), the renormalized matrix element at a non-perturbative scale μ_0 , and the SSF, we have computed the second moment of the pion non-singlet structure function in the continuum, but in the somehow unusual Schrödinger Functional scheme. The experimental data are usually parameterized in the more common $\overline{\text{MS}}$ scheme.

4 Results

The last step is to use the renormalization group equation to match the simulation data with the experimental data. The idea is to build a quantity that is scheme independent, and from which it is possible to switch to any preferred scheme. This quantity exists and for a matrix element it is called Renormalization Group Invariant (RGI)

matrix element, and it is nothing else than the integration constant of the renormalization group equation. In other words, in the limit $\mu \rightarrow \infty$ of the renormalized matrix element

$$\langle x \rangle_{\text{RGI}} = \langle x \rangle^{\text{scheme}}(\mu) f^{\text{scheme}}(\bar{g}^2(\mu)) \quad (20)$$

with

$$f^{\text{scheme}}(\bar{g}^2(\mu)) = (\bar{g}^2(\mu))^{-\gamma_0/2b_0} \exp \left\{ - \int_0^{\bar{g}(\mu)} \left[\frac{\gamma(x)}{\beta(x)} - \frac{\gamma_0}{b_0 x} \right] dx \right\}, \quad (21)$$

where \bar{g} is the renormalized coupling in the adopted scheme, $\gamma(g)$ is the anomalous dimension of the local operator, $\beta(g)$ is the β -function, and *scheme* stands for the preferred scheme used for the computation. Our preferred scheme to compute the non-perturbative evolution to a perturbative scale μ of the matrix element is the SF scheme:

$$\langle x \rangle_{\text{RGI}} = \langle x \rangle^{\text{SF}}(\mu) f^{\text{SF}}(\bar{g}^2(\mu)) \quad (22)$$

Once we have checked that the evolution is safely described, by a 2-loop anomalous dimension, and a 3-loop β -function (γ_1 and b_2 a re scheme dependent and must be computed in the SF scheme), it is possible to obtain

$$\langle x \rangle_{\text{RGI}} = 0.222(24). \quad (23)$$

From this number and from eq. (20) is possible to derive the $\overline{\text{MS}}$ number,

$$\begin{aligned} \langle x \rangle_{\text{quenched}}^{\overline{\text{MS}}}(\mu=2.4 \text{ GeV}) &= \langle x \rangle_{\text{RGI}} / f^{\overline{\text{MS}}}(\bar{g}^2(\mu)) = 0.30(3), \\ \langle x \rangle^{\text{experiment}}(\mu=2.4 \text{ GeV}) &= 0.23(2). \end{aligned} \quad (24)$$

The result seems to exceed the experimental value. The chiral extrapolation of the renormalized matrix element is done in the usual way quadratically in the pion mass. There are recent claims [14] that try to explain this discrepancy, already noticed by other collaborations (QCDSF, LHPC-Sesam), using chiral Perturbation Theory (χ PT), to go to zero quark mass. They modify, adding a phenomenological cut-off fitted by the data, the formula computed with χ PT and find then a good agreement with the experimental value. We believe that the value of the valence quark masses simulated are too big ($m_\pi \geq 500 \text{ MeV}$) to believe that χ PT can be trusted. Another source of systematic error is quenching. As an exercise, fix at some very low energy (500 MeV) the amount of momentum carried by valence quarks and follow its (2-loop) evolution in the quenched and in the unquenched

case. The ratio of the quenched over the unquenched case at a scale of 2.4 GeV is 1.12, if the input valence average momentum was 0.5, and 1.08 if it was 0.4. One obtains a bigger value in the quenched case as a consequence of the fact that, due to the faster running of the coupling in this case, the gluon bremsstrahlung is reduced with respect to the unquenched case. There are results from the QCDSF and LHPC-Sesam collaborations [3,15] that show an agreement between the unquenched and the quenched matrix element. Also in this case one should consider the rather high value of the sea quark masses used in the simulation. As a final comment, we mention that the main result of such a computation on the lattice, is the *Renormalization Group Invariant* (RGI) matrix element. The reason is that RGI quantities can be used directly in other regularization schemes.

References

1. S. Capitani *et al.*, Nucl. Phys. B Proc. Suppl. **73**, 288 (1999); C. Dawson *et al.*, Nucl. Phys. **514**, 313 (1998).
2. S. Capitani *et al.*, Nucl. Phys. B Proc. Suppl. **79**, 548 (1999).
3. D. Dolgov *et al.*, Phys. Rev. **66**, 034506 (2002).
4. P.H. Ginsparg, K.G. Wilson, Phys. Rev. **25**, 2649 (1982); M. Lüscher, Phys. Lett. **428**, 342 (1998).
5. H. Neuberger, Phys. Lett. **417**, 141 (1998); **427**, 353 (1998).
6. D. Kaplan, Phys. Lett. **288**, 342 (1992); V. Furman, Y. Shamir, Nucl. Phys. **439**, 54 (1995).
7. P. Hasenfratz, F. Niedermayer, Nucl. Phys. **414**, 785 (1994); P. Hasenfratz, Nucl. Phys. B Proc. Suppl. **63**, 53 (1998).
8. A. Bucarelli, F. Palombi, R. Petronzio, A. Shindler, Nucl. Phys. **552**, 379 (1999).
9. M. Guagnelli, K. Jansen, R. Petronzio, Nucl. Phys. **542**, 395 (1999).
10. M. Guagnelli, K. Jansen, R. Petronzio, Phys. Lett. **457**, 153 (1999).
11. M. Guagnelli, K. Jansen, R. Petronzio, Phys. Lett. **459**, 594 (1999).
12. M. Guagnelli, K. Jansen, R. Petronzio, Phys. Lett. **493**, 77 (2000).
13. M. Lüscher, R. Narayanan, P. Weisz, U. Wolff, Nucl. Phys. **384**, 168 (1992); K. Jansen *et al.*, Phys. Lett. **372**, 275 (1996); S. Capitani, M. Lüscher, R. Sommer, H. Wittig, Nucl. Phys. **544**, 669 (1999).
14. W. Detmold *et al.*, Phys. Rev. Lett. **87**, 172001 (2001).
15. S. Capitani *et al.*, Nucl. Phys. B Proc. Suppl. **106**, 299 (2002).